

## Article

# Assessment of Future Climate Change Impacts on Groundwater Recharge Using Hydrological Modeling in the Choushui River Alluvial Fan, Taiwan

Thi-My-Linh Ngo <sup>1</sup>, Shih-Jung Wang <sup>1,2,\*</sup>  and Pei-Yuan Chen <sup>3</sup> 

<sup>1</sup> Graduate Institute of Applied Geology, National Central University, 300 Zhongda Rd., Zhongli District, Taoyuan City 32001, Taiwan; linh.ntmhcm@gmail.com

<sup>2</sup> Department of Earth Sciences, National Central University, 300 Zhongda Rd., Zhongli District, Taoyuan City 32001, Taiwan

<sup>3</sup> Graduate Institute of Hydrological and Oceanic Sciences, National Central University, 300 Zhongda Rd., Zhongli District, Taoyuan City 32001, Taiwan; pychen@ncu.edu.tw

\* Correspondence: sjwang@ncu.edu.tw

**Abstract:** This research delves into the crucial role of groundwater in underpinning ecosystems and human resilience amidst drastic and unpredictable climate change, particularly as water resources face increasing sustainability concerns due to population surges and climate change. Utilizing a combined approach of SWAT-MODFLOW models, we estimate the streamflow discharge and groundwater recharge in the Choushui River Alluvial Fan, Taiwan. These models allow evaluation of the distribution and proportion of recharge areas as well as the accuracy and the potential influence of future climate change scenarios on groundwater recharge. The findings show a strong correlation between the simulation and actual observations, evidenced by the Nash–Sutcliffe model efficiency coefficients (NSE) of 0.920 and 0.846 for calibration and validation in the Choushui River, and 0.549 and 0.548 for the Pei-Kang River, respectively. The model demonstrates a reliable representation of the watershed response, supported by robust statistical performance. The analysis reveals the variable impacts of climate change on groundwater recharge, dependent on the chosen scenario and period. Some scenarios indicate that the maximum observed increase in groundwater recharge is 66.36% under the RCP2.6 scenario in the long-term period (2061–2080), while the minimum observed increase is 29.67% under the RCP4.5 scenario in the initial time frame; however, all demonstrate a decrease ranging from 23.05% to 41.92% across different RCPs in the impact of climate change over time, suggesting a potential long-term decrease in the impact of climate change on groundwater recharge. This study provides indispensable insights into the spatial hotspots in the top fan and the potential range of impact rates of climate change on groundwater recharge, underscoring the importance of continuous research and the thorough evaluation of multiple scenarios. Moreover, we establish a primary framework for using a top-ranked MIROC5 projection of general circulation models (GCMs) to delineate an essential premise that facilitates the advanced exploration of alternative scenario augmentations, bolstering the comprehensive investigation of climate change impacts on groundwater recharge. It is proposed that these findings serve as a guidepost for sustainable water resource management and policy-making in the face of climate change and escalating water demand.

**Keywords:** hydrological modeling; climate change impact; surface water; groundwater recharge; SWAT-MODFLOW



**Citation:** Ngo, T.-M.-L.; Wang, S.-J.; Chen, P.-Y. Assessment of Future Climate Change Impacts on Groundwater Recharge Using Hydrological Modeling in the Choushui River Alluvial Fan, Taiwan. *Water* **2024**, *16*, 419. <https://doi.org/10.3390/w16030419>

Academic Editors: Xander Wang and Lirong Liu

Received: 3 January 2024

Revised: 23 January 2024

Accepted: 25 January 2024

Published: 27 January 2024



**Copyright:** © 2024 by the authors. Licensee MDPI, Basel, Switzerland. This article is an open access article distributed under the terms and conditions of the Creative Commons Attribution (CC BY) license (<https://creativecommons.org/licenses/by/4.0/>).

## 1. Introduction

Groundwater is an essential part of the climate system [1], but many of the possible implications of climate change are unknown since the system is complex [2]. Understanding the potential implications of climate change on groundwater resources is crucial for ensuring the long-term viability of groundwater management in a changing environment.

Moreover, groundwater is significant for supporting ecosystems and assuring human resilience to significant and unpredictable climatic change, especially as surface water systems become more unsustainable due to fast population expansion and climate change. To manage water resources sustainably, locating the recharge in certain areas where groundwater substantially contributes to the water supply is important. Furthermore, the climate is the key factor driving spatial and temporal recharge variation. Precipitation and temperature are key climatic factors that determine the availability and movement of water in the environment, which in turn influences groundwater recharge rates despite the fact that there are other pathways for groundwater recharge. To accomplish this work, one must deal not only with the hydrology of the surface but also with the subsurface. The inappropriate management and excessive usage of diverse water supply portions influence the long-term viability of the watershed and the environments it supports. It would be helpful for the authorities to know where and when groundwater recharge is expected to decline so that they can make appropriate provisions and establish a proper plan for managing water resources.

There have been very few investigations into the links between climate change and groundwater until recently [3–8]. The inadequacy in comprehending groundwater response to climate change forcing is partly accounted for by the challenges associated with exploring the nature and features of subsurface water. Water cycle vulnerability assessments and management for long-term use will come to a standstill unless we increase our knowledge of hydrology systems. Quantifying water resources on a regional scale has required the development of various strategies and approaches, such as large-scale watershed models. Because the vast majority of models focus their attention primarily on surface water [9–11], they consequently disregard the accessibility of groundwater as well as the substantial influence it has on surface water [12–14]. A new generation of models use an approach that is more complex in linking the hydrologic processes that occur on the ground surface and underneath it, such as ParFlow [15], GSFLOW [16], SWAT-MODFLOW [17], HydroGeoSphere [18], CATHY [12], and FEFLOW [19]. Significantly, modeling is an essential tool for comprehending the circumstances of the past and the present, as well as for forecasting and, eventually, exercising control over the future outcomes of geophysical and earth systems, which include climate patterns, land use, soil profile, and processes. This is further substantiated by The Soil and Water Assessment Tool (SWAT) [20,21], which was recognized as the most common model in watershed management, soil, and water from a list of 73 different models [22–25].

SWAT has historically focused on surface operations since it only provides a rudimentary depiction of groundwater dynamics, and its outcome is not spatially comprehensive. Therefore, this study expanded the soil profile in the root and vadose zones. The surface water model uses DEM to divide the basin into sub-basins; each sub-basin is further separated into hydrologic response units (HRUs), possible soil-type variations, land use, and slope characteristics. In addition, integrating the MODFLOW–NWT (a Newton–Raphson formulation for MODFLOW-2005) [26] into the framework of the SWAT model can significantly expand both models' utility. SWAT is known for its ability to simulate complete rainfall runoff and water quantity, while MODFLOW is known for its rigorous modeling of subsurface flow. Since each model has advantages and disadvantages of its own, Sophocleous et al. [27] were the first to suggest combining the beneficial features of the models. MODFLOW has been used in various research projects to analyze groundwater through the surface water supply [28,29]. The approach of the groundwater module converts groundwater level fluctuation with hydraulic conductivity and storativity. MODFLOW can be combined with surface water models such as SWAT to acquire spatially and temporally variable recharge rates. Using the SWAT may simulate recharge from the surface because MODFLOW would not mimic land and atmosphere interactions, agricultural operations, or surface runoff [30,31]. Therefore, the groundwater flow calibration with an automatic PEST approach in MODFLOW may provide reliable results of the recharge dynamic of

SWAT. These simulations are being utilized to find solutions to various groundwater management-related issues.

The widespread use of general circulation models (GCMs) in groundwater assessment and prediction highlights the importance of climate patterns to groundwater. Dry circumstances may have the reverse effect, leading to decreased recharge and storage, whereas wet conditions almost always result in greater recharging and storage [32,33]. McKenna and Sala [34] assessed the anticipated changes in recharge under future climate predictions. They found a net gain owing to the expected increases in precipitation countering a reduction in recharge due to increasing temperatures. Maxwell et al. [35] demonstrated that aquifers impact the atmosphere, particularly in regions with shallow aquifers where surface water and groundwater interact. The Intergovernmental Panel on Climate Change (IPCC), in its Fifth Assessment Report (AR5), summarized the lack of subsurface and climate studies by introducing the innovations and consequences of its methodology, which expands study across sectors and geographies. The AR5 considers more severe significant effects on humanity and societal factors from climate-related risks and vulnerable societies and systems [2]. Furthermore, a paucity of research relating to groundwater has been indicated in the AR5, with “very few studies on the climate change’s impact on groundwater” [36,37].

Building on the need for in-depth study, there is a possibility that evapotranspiration (ET) will impede penetration below the root zone; thus, slight rainfall is hard to percolate to groundwater recharge. The quantity of rain is not the only factor that determines the amount of water reabsorbed by the ground; its intensity is also essential [38,39]. It was discovered that projected recharge estimates in a future climatic scenario are quite sensitive to the amount of rainfall that occurs [40,41]. Even in karst terrain, less than 15 mm of precipitation is considered inconsequential for recharge, whereas 30 mm or more leads to considerable groundwater recharge [42]. In a recent study by Hersi et al. [8], in a data-scarce catchment with steep slopes, a 15% reduction in rainfall led to a decrease in recharge by up to 24%, whereas in gentler slope areas, a 25% increase in rainfall correlated with an increase in recharge by up to 123% compared with the baseline period. Therefore, locations at which rainfall intensity would be anticipated to grow may witness future recharge increases, providing rainfall intensity does not surpass soil capacity and prohibits further groundwater recharge. In addition, Meixner et al. [43] found that different recharge processes react differently to climate change, and an area’s susceptibility to climate change relies on its groundwater recharge. Diffuse recharge is anticipated to diminish for the several layers below the subsurface due to declining precipitation, rising temperature, and increased ET [44]. Alterations in the flow behavior between the land surface and subterranean aquifers may potentially constitute the first and most visible direct groundwater-related repercussions of climatic variability. The connection between surface water and groundwater is complex and multidimensional, with the climate significantly impacting geological formations, landforms, and physical variables [44]. The impact of climate manifests through its control over precipitation patterns, erosion dynamics, and the permeability characteristics of soil and rock formations, underscoring the paramount importance of comprehending and integrating these interdependencies into water resource management practices. The systems are connected by a shared link comprising recharge and outflow, and the interaction between them is an essential component of the hydrologic cycle [45,46]. The most effective water resource management strategies for augmenting the diminishing surface and groundwater reserves, as underscored by Karki et al. [7], emphasize the criticality of evaluating climate change impacts in heavily irrigated watersheds through integrated surface and groundwater modeling. Concurrently, a forecasted decrement in groundwater levels may exacerbate the strain on the region’s water resources, which are vital for irrigation purposes, and consequently pose a risk to the sustainability of agricultural practices. Furthermore, groundwater recharge rates are known to be intricately linked to a range of environmental factors. As highlighted by Moeck et al. [47], these rates are not only highly dependent on precipitation and temperature but are also significantly influenced by vegetation cover and soil structure. This interdependency underscores

the need for comprehensive models that can accurately account for these diverse factors when assessing groundwater recharge under varying climatic conditions. To find solutions to groundwater management-related issues, the objectives of this study are to employ SWAT-MODFLOW models, which estimate streamflow discharge and assess the impact of climate change scenarios' influences on groundwater recharge in the future to identify the most effective and practical water resource management strategies for refilling the severely reduced surface water and groundwater supplies.

## 2. Materials and Methods

### 2.1. Study Area

The Choushui River Alluvial Fan (CRAF) is located in the central western region of Taiwan and encompasses the downstream section of the Choushui River watershed. This area predominantly includes the northern part of Changhua County, situated north of the Choushui River, and Yunlin County, which lies south of the river (Figure 1). This study covers an area of 2013.33 km<sup>2</sup> that has a subtropical monsoon climate that characterizes central Taiwan, which is close to the Tropic of Cancer. The pluvial period extends from May to October, constituting 79% of the total annual precipitation. In contrast, the arid phase persists from November to April of the subsequent year, owing to the interrelation between typhoons and diurnal heat convection. A decline in annual rainfall can be observed across the gradient from the highlands to the coastal regions. In the hilly eastern area, annual precipitation may exceed 1825 mm; with a range extending from 1120 to 2808 mm; centrally, within the alluvial plain, rainfall varies between 795 and 1994 mm, averaging at 1350 mm; and along the shore, the range narrows to 467 to 1772 mm, with an average of 1156 mm (Water Resources Agency, Taipei, Taiwan, 2009–2022). The annual average temperature is around 21.9 °C.

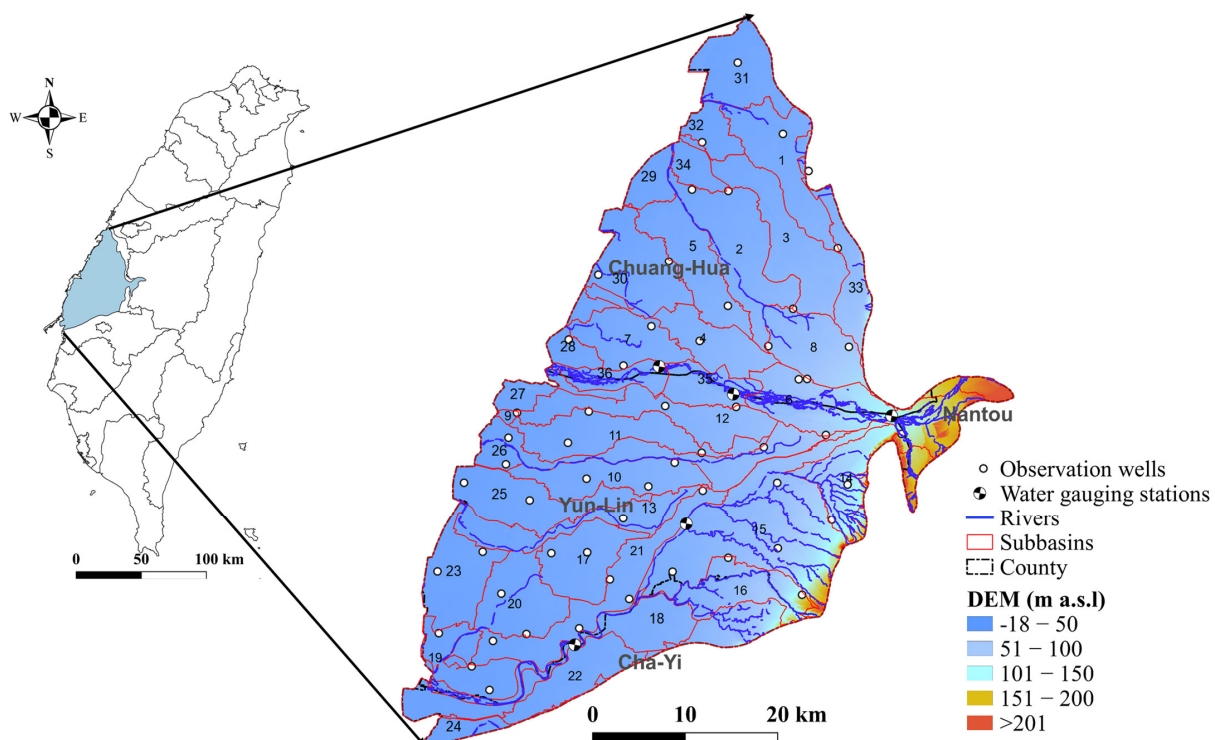


**Figure 1.** Location of the Choushui River Alluvial Fan and the delineation in SWAT and MODFLOW. Numerical identifiers in the figure correspond to each sub-basin.

The mean watershed elevation is 100 m above mean sea level (AMSL), ranging from –18 to 460 m. The land use is dominated by arable agricultural land, constituting approximately 69% of the total area. The remaining land is diversified among forest, pastures, and

wetland areas, each constituting 1%, 1%, and 3%, respectively, as well as pasture and various urban categories: urban—industrial (7%), urban—high density (2%), urban—medium density (11%), and urban—low density (1%). Additionally, water bodies represent 6% of the land use. Soil types in the vadose zone are loam, sandy clay loam, fine sand, etc. The groundwater storage system along the CRAF is Taiwan Island's biggest alluvial fan and has the most copious groundwater reserves. For instance, crop seedlings require a water supply for a considerable time. In cases where surface water availability is inadequate, agricultural water demand may necessitate the extraction of groundwater resources. However, the rampant exploitation and utilization of groundwater resources over a prolonged period have led to a drastic decline in the groundwater table, resulting in severe land subsidence, seawater intrusion, and soil salinization [48]. Aquaculture, agricultural irrigation, industrial growth, and heavy water consumption cause significant groundwater outflow over extended periods, which causes groundwater levels to continue to fall. Hsu [49] discovered that the groundwater level has been declining since an initial observation in 1968 after analyzing the groundwater level data from the mixed-layer observation wells in the Yunlin region on the southern edge of the CRAF.

Moreover, as indicated by Ke [50], Changhua and Yunlin counties have 40% of Taiwan's irrigation areas. Changhua County used 2272 million m<sup>3</sup>/year of water from 2004 to 2009, including 1423 million m<sup>3</sup>/year of surface water and 849 million m<sup>3</sup>/year of groundwater. According to the Consuming Water Resources Database, in this county, agricultural demands has access to 98% of the available surface water and 29% of the groundwater reserves. Concurrently, alternative sectors leverage a considerable 71% of the groundwater, of which aquaculture singularly consumes 43%. Over in Yunlin County, a substantial 96% of irrigation necessities are satisfied by surface water resources. Moreover, the groundwater here predominantly underpins local industries and aquaculture, accounting for 36% and 26%, respectively. Without abundant groundwater, surface water barely covers agricultural water needs. This suggests the necessity of controlling surface water and groundwater in the studied region. Therefore, it is imperative to comprehend the potential quantity of water that will be restored in the forthcoming period to formulate effective management strategies.

## 2.2. Methodology

### 2.2.1. SWAT Model Set-Up

The QSWAT3 version 1.5 interface was employed, a component integrated within the Quantum Geographic Information System (QGIS) 3.22.10 platform, exhibiting compatibility with the latest iteration of the SWAT Editor. The investigative approach incorporated various input parameters for the SWAT model, including topographical features, land utilization, soil composition, climatic conditions, well locations, and stream discharge data. To synthesize the SWAT model before calibrating and validating it to display streamflow outcomes under climate changes, QSWAT permitted the spatial definition of the catchment area and the variables impacting the watershed hydrological features.

The watershed was divided into 36 sub-basins (Figure 1), where the whole sub-basin drains to the sub-basin outlet, based on the 30 m pixel size digital elevation model (DEM) provided by Academia Sinica (2019). HRUs represent a homogeneous land area within a watershed, delineated based on the unique combination of land use, soil type, and slope. It is assumed that each HRU exhibits a uniform response to hydrological processes, such as precipitation, evapotranspiration, surface runoff, and groundwater recharge. For the construction of HRUs, a soil map was employed, derived from the Construction and Planning Agency Minister of the Interior Database (2020), featuring a 30 m grid resolution. Land-use classification adhered to the United States Geological Survey (USGS) database, requisite for SWAT model preparation (shown in Figure 2). Slope categories were stratified into three distinct bands (2%, 2–6%, and >6%), contingent upon the field properties, such as soil infiltration capacity and land utilization. The slope attributes demarcate discrete gradations, for instance, delineating overflow or drainage channels to eliminate excess water from cultivated regions; even in areas with a modest slope of 2–6%, farming grounds may infiltrate 10% of the annual rainfall [51]. The slope distinguishes

levels based on field structures like soil infiltration and land utilization. Groundwater recharge is controlled not only by hydrologic processes but also by the physical properties of the soil profile and the land surface. Factors such as urbanization and climate change can significantly affect recharge rates. Based on the combination of land use, soils, and slope, the catchment was discretized into 2568 HRUs. By dividing a watershed into multiple HRUs, the hydrological model can more accurately simulate the spatial variability of these processes.

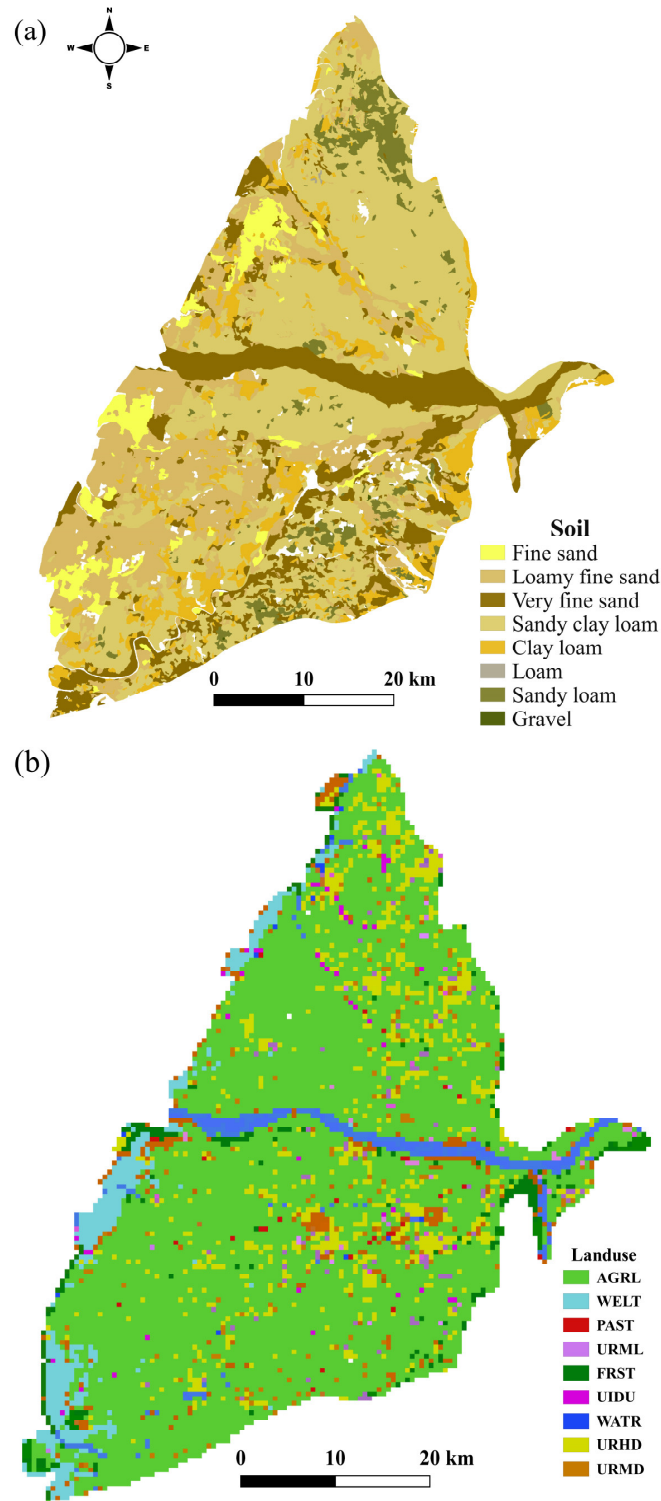


**Figure 2.** Distribution and proportion of (a) soil and (b) land use, after classification employing the HRU delineation defined within the SWAT framework.

The primary objective of soil classification is to transform user-supplied soils into SWAT databases (or grid properties). Following the process, Taiwan's soil taxonomy was converted into Food and Agriculture Organization (FAO, Rome, Italy) terminology. Consequently, the relevant United States Department of Agriculture (USDA, Washington, USA) words are specified. Moreover, the soil profile database was considered following the depths of the vadose zone to the shallow aquifer. Then, each soil-type hydrologic soil group was determined. The physical characteristics of soil are mainly shown in Figure 2.

The streamflow and velocity were measured to determine the flow rate of surface water bodies. As a result, surface water levels are included in the observed data gathered monthly at five stations, shown in Figure 1. We postulated that automatic irrigation management was implemented within the HRUs, as ascertaining the precise water quantity supplied for irrigation proved challenging. Infiltration estimation was conducted utilizing the curve number method (USDA, 1972) [52], which is contingent upon land use, soil permeability, and hydrological conditions. Precipitation drives the vadose zone soil water budget, which recharges groundwater. However, precipitated water is susceptible to various processes, including evaporation, interception, and surface runoff. These processes are influenced by rainfall intensity, surface runoff, and temperature. There is also a possibility that some of the water may seep into the ground, where the plant roots will absorb it and then exhale it as water vapor via the leafy covering of the plants. The activities of absorption and evaporation, as well as potentially significant processes like streamflow and throughfall, all affect recharge, which is influenced by land use. When the water volume within a terrain surpasses its retention capacity, the percolating water is subject to one of two possible pathways: channeled to streams through lateral flow or continuing its downward movement into the groundwater. Hence, the interplay of diverse parameters and complex conditions inherent in the calibration process plays a crucial role in understanding the impact of climate change on groundwater recharge.

### 2.2.2. MODFLOW-NWT Model Set-Up

A transient MODFLOW-NWT model is constructed for the CRAF with a hydro-stratigraphic shallow aquifer and a discretization of grid cells  $500\text{ m} \times 500\text{ m}$  (Figure 3). The data sources utilized in the first layer (shallow aquifer), including the hydraulic conductivity, storativity, and aquifer thickness, were provided by the Water Resources Agency, Ministry of Economic Affairs, Taiwan [53]. For the model set-up, the interpolation of storativity and hydraulic conductivity via the Kriging method was employed and subsequently validated. The validation process involved comparing the Kriged estimates against a set of observed data points that were withheld from the initial interpolation process. The performance of the Ordinary Kriging was quantified using the RMSE (NSE), which resulted in values of 2.45 m (0.89) for hydraulic conductivity and 0.30 m (0.90) for storativity, respectively. Furthermore, cross-validation techniques were also implemented, where each data point was removed in turn, and its value was predicted using the remaining data points. The predicted values were then compared with the actual observed values, contributing to the confidence in the Kriging method's predictive capability. The boundaries of the research domain encompass hydrological attributes, such as groundwater subdivisions and physical elements. In Figure 3, the left-hand border is configured as a specified head, wherein the head value along the edge is established at a known value. The upper portion of the right-hand boundary is designated as a no-flow condition where the flow across the boundary is zero. The lower segment of the right-hand side is assigned a general head status, owing to the gradient disparity between a specified head external to the boundary and the head calculation at a nodal point situated on or proximate to the boundary. It is postulated that the entirety of the water percolated from the SWAT model will ultimately contribute to the recharging of the shallow aquifer. The mean annual recharge rate, derived from SWAT outcomes spanning 1989 to 2017, was employed as input data for the recharge package. The transient model's calibration was facilitated by 62 head observations (shown in Figure 1) amassed between 2005 and 2011 and validated from 2012 to 2017.

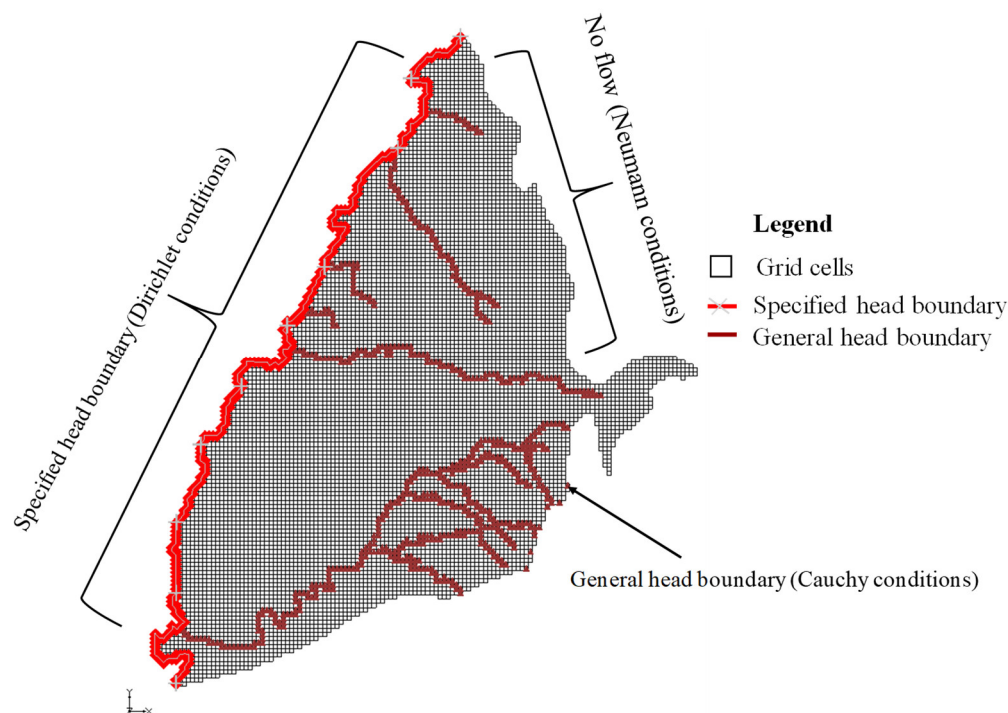


**Figure 3.** Boundary conditions set-up in MODFLOW model.

### 2.3. Model Calibration and Validation Procedure

#### 2.3.1. SWAT Calibration

Assessment of the hydrologic balance is a prerequisite for SWAT application and is often presented independently of the analysis focal point. Stream discharge performance was evaluated by employing the sequential uncertainty fitting algorithm (SUFI2) [54], integrated within the SWAT-CUP software suite. This study utilized the most recent iteration of the software, version 5.1.6.2. The Nash–Sutcliffe efficiency metric [31] served as the primary objective function throughout the calibration process. The data used for calibration spanned from January 1989 to December 2017, encompassing monthly discharge measurements and a model warm-up period before the commencement of the calibration process. The initial value ranges for basin-wide and sub-basin parameters associated with streamflow were ascertained. Additionally, it should be noted that the multiple monitoring stations within the study area exhibited hydrological interconnectivity. Firstly, the locations of these stations in Choushui River are the outflow of sub-basins 6, 35, and 36, respectively (marked in Figure 1). Secondly, two gauging stations are situated in the Pei-Kang River, which includes sub-basin 15 (Tun-Kun station) and sub-basins 16 and 18 (Pei-Kang (2)).

Considering Chun-Yun station is positioned upstream of the top fan (sub-basin 6), its water flow affects Chi-Chou and Tzu-Chiang stations, which are located downstream of Chun-Yun station (sub-basins 35 and 36, respectively). Therefore, the inlet source flow from upstream was what the Chun-Yun station (sub-basin 6) was discharging as its discharge. The simulated discharge of station Chi-Chou was first calibrated by conducting five iterations with 500 simulations each. Two stations of the Choushui River cannot be calibrated simultaneously since the Tzu-Chiang station does not have data after 2000, which was used to provide a preliminary estimate. After the last iteration for station Chi-Chou, the sub-basin parameters for the area station Tzu-Chiang were fixed, and the final ranges of the basin-wide parameters were utilized in the subsequent calibration of station Tzu-Chiang. After the Chi-Chou calibration was finished and the parameters were set, the simulation was run from January 2005 to December 2011, with the first 16 years serving as a warm-up period (1989–2005). After calibration, the model was tested using a separate dataset, then validated from January 2012 to December 2017. This methodology ensured that the sub-

basin-level values represented each station’s respective regions. Additionally, the water stress threshold required manual calibration so that a simulation of the auto-irrigation quantity could be carried out. The method for calibration and validation was also similar to the Pei-Kang River. These metrics included the Pearson correlation coefficient ( $r$ ), the coefficient of determination ( $R^2$ ), the Nash–Sutcliffe efficiency coefficient, and the percent bias ( $P_{bias}$ ) based on the best cognitive remedy. The simulation uncertainties of hydrologic response were analyzed by optimal values auto-calibration parameters close to observed streamflow to build a fundamental prediction of future development scenarios (shown in Table 1). However, within the calibration process of complex hydrological models like SWAT, a negative adjustment factor does not necessarily denote a negative physical quantity of water. Instead, it functions as a calibration index to fine-tune the model’s output to match observed data. This index can offset other model parameters or assumptions that might have been initially overestimated.

**Table 1.** Initial ranges and calibrated values for the parameters specified for SWAT model.

Parameters	Description	Initial Range	Calibrated Values	
			Sub-Basin: 6, 15 (Upstream)	Sub-Basin: 16, 18, 35, 36 (Downstream)
CN2.mgt	Initial SCS runoff curve number for moisture condition II	−0.3 to 0.3	−0.279	0.137
Alpha_BF.gw	Baseflow alpha factor for shallow aquifer (days)	0–1	0.453	0.6953
ESCO.bsn	Soil evaporation compensation factor	0–1	0.466	0.931
EPCO.bsn	Plant uptake compensation factor	0.01–1	0.163	0.254
SOL_AWC.sol	Available water capacity of the soil layer (mm H <sub>2</sub> O / mm soil <sup>−1</sup> )	−0.8 to 0.8	−0.674	0.786
SOL_BD.sol	Moist bulk density (gcm <sup>−3</sup> )	−0.2 to 0.2	−0.067	−0.025
GW_DELAY.gw	Groundwater delay (days)	0–200	116.12	121.23
SURLAG.bsn	Surface runoff lag coefficient (days)	1–10	1.747	6.379
GW_REVAP.gw	Groundwater “revap” coefficient	0.02–0.1	0.092	0.0313

### 2.3.2. MODFLOW Calibration

In order to calibrate MODFLOW, parameter values were compared against the measurements of groundwater table, and the results were utilized to perform a combination of auto-calibration using the PEST pilot method and manual calibration. To initiate a process for calibrating the model based on pilot points, this will be supplemented by applying geostatistical-based restrictions on the values of the parameters via the utilization of the regularization capabilities provided by the PEST. The time periods that were used for the model’s “warm-up” period (initial head for calibration period) lasted for two years (2003–2004). The periods employed for SWAT were also utilized for the calibration and validation processes of the MODFLOW model. After each iteration of a PEST run, the PEST optimization algorithm (the Levenberg–Marquardt method [55]) adjusted the values of the model parameter variables to optimize the value of the objective function. Therefore, the hydraulic conductivity and storativity were two parameters automatically calibrated by the PEST approach for 10,000-time iterations, and the pumping rate was manually calibrated, ranging between 0.5 billion and 1 billion m<sup>3</sup>/year, following the Central Geological Survey, Taiwan.

#### 2.4. Climate Change Scenarios

The accuracy of climate risk assessments mainly relies on the forecasts that GCMs make on the future climate. There are many GCM datasets available; however, it is not practical nor required to employ all of the datasets available for undertaking climate risk assessments. CMIP5 (Coupled Model Intercomparison Project Phase 5) contains the results of several different GCMs that have been constructed, continually improved, and reported. Lin and Tung [56] revealed that GCM ranking for a single weather station using the weighted average ranking (WAR) [33] and demerit point system (DPS) techniques independently ranks all GCMs that are available for use with the particular weather station. As a result, the WAR approach and the DPS analysis both considered the recommendation list MIROC5, one of the GCMs, which ranks first on the central climatic zonation when the suggestion list was used to reconstruct the historical mean precipitation and temperature trend for the study area. Analysis of the MIROC5 dataset was carried out by The University of Tokyo's Atmosphere and Ocean Research Institute, the National Institute for Environmental Studies, and the Japan Agency for Marine–Earth Science and Technology. Such frameworks, including the introduction of the MIROC5 projection of GCMs in this study, lay the groundwork for its future utilization and underscore this study's advanced holistic assessment of future groundwater recharge impacts.

Climate data, comprising the daily precipitation and temperature data with the distribution stations inside the whole watershed with the finest practical spatiotemporal resolutions of five kilometers over 100 years, were selected to accommodate the historical and future climatic conditions of catchment features, which Taiwan Climate Change Information Knowledge Platform (TCCIP) downscaled from AR5 [57]. The finer resolution of detail can capture microclimatic variations that might be lost at coarser scales, which is particularly important in complex terrain where climate impacts can vary significantly over short distances. It also allows for accounting for possible changes in land use, urbanization, and other factors that could affect hydrological responses at these finer scales. The scenarios were developed to predict the effect of climate change using 45 years of actual historical climate data as a reference. Throughout the research spanning 100 years, each simulation parameter was adjusted accordingly. This research aims to simulate and observe the general behavior of the system in response to variations in the model's input parameters based on the commonly accepted predictions. These potential developments have been attempted to be captured by RCP2.6, RCP4.5, RCP 6.0, and RCP 8.5, which are representative concentration pathways employed in climate research to delineate distinct trajectories of greenhouse gas concentrations. These scenarios encompass a spectrum of emissions scenarios, spanning from stringent mitigation efforts (RCP2.6) to moderate (RCP4.5, RCP6.0) and high-emission scenarios (RCP8.5). By capturing a range of potential future climate conditions, these pathways facilitate rigorous analysis and evaluation of the possible climatic impacts associated with varying greenhouse gas concentration trajectories. The concentrations in the near-term (2021–2040), mid-term (2041–2060; 2061–2080), and long-term (2081–2100) are referred to by the numerical values of the RCPs.

### 3. Results and Discussion

#### 3.1. Parameters Sensitive Analysis of SWAT

In this research, before the model was ready for use in any scenario analysis, all these sensitive input parameters were considered during the calibration and validation steps included in the watershed modeling. Under the assumption that both local and global sensitivity analyses yield reliable sensitive input parameters when their values approach zero, parameters are deemed sensitive. Table 2 presents a comprehensive analysis of the findings when comparing local and global sensitivities. For each variation in the SWAT input parameters, 500 iterations were run through the simulation to comprehend the most sensitive parameters and control the runoff when calibrating the model. The concept of local sensitivity illustrates how sensitive a variable is to changes in a single parameter while requiring that other parameters remain unchanged at some values. Global sensitivity refers

to the average changes that will occur in the objective function as a direct consequence of changes made to each parameter when all of the other parameters are also being altered. The evaluation of the sensitive parameters in SUFI-2 is carried out by using the *t*-stat values, and a parameter is considered more sensitive if it has a larger absolute *t*-stat value. *p*-values are utilized to assess whether or not a parameter is significant, with significance being conferred on the parameter if the *p*-values are near zero. Therefore, there were five parameters (i.e., CN2, GW\_delay, Alpha\_BF, SOL\_BD, SOL\_AWC), which emerged as the primary determinants in the regulation of surface runoff.

**Table 2.** The sensitivity analysis results during calibration.

No	Parameters	Local Sensitivity		Global Sensitivity	
		<i>t</i> -Stat	<i>p</i> -Value	<i>t</i> -Stat	<i>p</i> -Value
1	r_CN2.mgt	−8.4630	0.0000	−4.1010	0.0010
2	v_Alpha_BF.gw	4.8934	0.0017	−0.0560	0.4782
3	v_ESCO.bsn	2.9230	0.0084	0.9840	0.1754
4	v_EPCO.bsn	3.1308	0.0060	1.1080	0.1482
5	r_SOL_AWC.sol	4.6790	0.0213	14.7550	0.0000
6	r_SOL_BD.sol	−1.8920	0.0455	−33.6700	0.0000
7	v_GW_DELAY.gw	9.9718	0.0000	−1.6530	0.0663
8	v_SURLAG.bsn	−1.8720	0.0469	0.4660	0.3261
9	v_GW_REVAP.gw	2.3410	0.0219	0.0640	0.4751

v\_ denotes replacing a parameter value with a specified one, and r\_ means multiplying the existing parameter value by (1 + a specified value).

### 3.2. SWAT Model Transient Performance

The calibration is more reliably described physically by comparing the observation and the simulation of the typical streamflow in a large-scale distributed watershed. Therefore, the patterns of the hydrographs of the simulated streamflow for four stations (Figures 4 and 5) were comparable to the observed data for those locations. The statistical performance values for the monthly stream discharge (Table 3) were determined in four stations, including Tzu-Chiang, Chi-Chou, Tun-Kun, and Pei-Kang (2). The findings showed that the calibrated and validated SWAT model in the Choushui River were 0.920 and 0.846, respectively, for the Nash–Sutcliffe model efficiency coefficients. For the case of the Pei-Kang River, the NSE values for calibration and validation were 0.549 and 0.548, respectively. The NSE values for calibration and validation in the Pei-Kang River revealed a small efficiency coefficient because of an unknown data source upstream; however, it demonstrated generally good statistical performance for the temporal pattern of streamflow, with RMSE, NSE, R<sup>2</sup>, and P<sub>bias</sub>. The streamflow in the Choushui River was accurately simulated compared with the observed values because the upstream inlet of the Chang-Yun bridge controlled it. The results showed that the SWAT model adequately reproduced the streamflow hydrographs throughout the calibration and validation period and demonstrated that it could more accurately predict the high peak flow event. The precise simulation of surface runoff can contribute to diminishing uncertainty when analyzing the repercussions of prospective climate alterations on groundwater replenishment processes.

**Table 3.** Performance of the quantitative indicators for monthly discharge at sub-basin outlets during the SWAT-CUP calibration and validation (in brackets) periods.

Outlets	Pearson Correlation Coefficient	RMSE (m)	R <sup>2</sup>	P <sub>bias</sub> (%)	NSE
Tzu-Chiang	0.979 (0.971)	2.742 (1.194)	0.959 (0.943)	−0.003 (−0.131)	0.942 (0.866)
Chi-Chou	0.959 (0.930)	0.020 (0.114)	0.920 (0.865)	−0.001 (0.010)	0.920 (0.846)
Tun-Kun	0.865 (0.857)	0.354 (0.056)	0.749 (0.734)	0.289 (−0.029)	0.549 (0.469)
Pei-Kang (2)	0.865 (0.857)	0.354 (0.605)	0.749 (0.679)	0.289 (0.181)	0.549 (0.548)

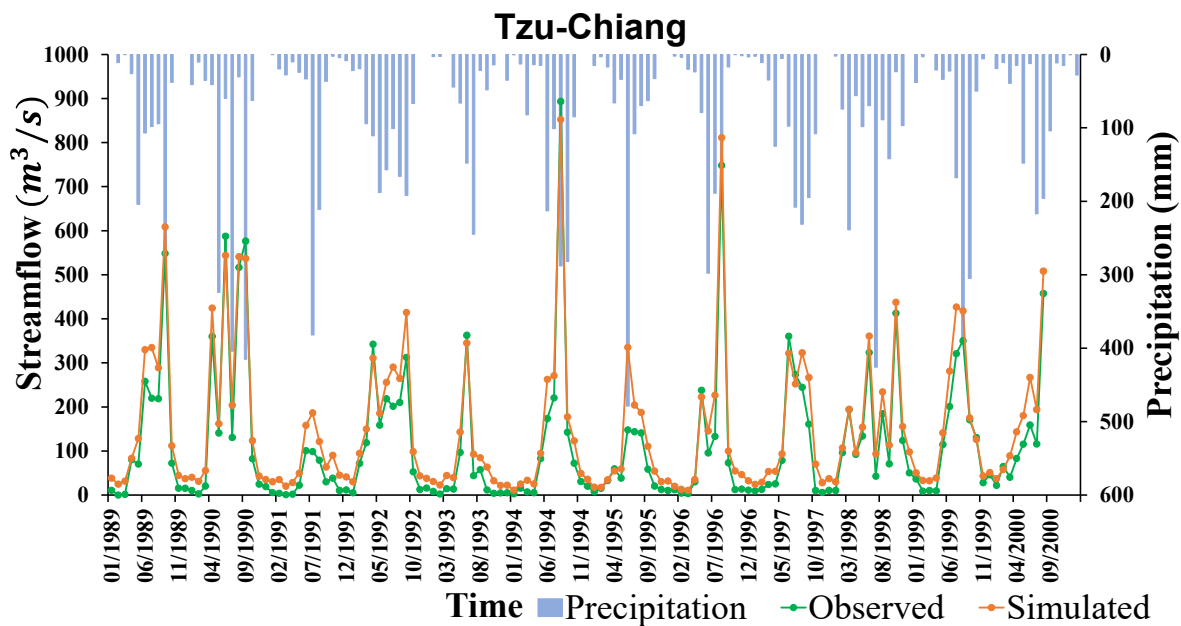


**Figure 4.** The hydrographs illustrate the monthly best simulated, observed streamflow, and precipitation at the outlet of the Tzu-Chiang bridge throughout the calibration time (1989–1994) and the validation period (1995–2000).

### 3.3. MODFLOW Transient Model Calibration

Groundwater level observation data series are compared with the simulated head of four boreholes, for example, as shown in Figure 6. They demonstrate that the model captures the general trends of the groundwater levels with commendable precision, which is particularly evident during periods of significant hydrological stress. They address the need for continued monitoring and model refinement to account for the dynamic nature of groundwater systems and the uncertainties inherent in model predictions. Following each iteration of a PEST run, the optimization algorithm will modify the values of the model parameter variables in order to obtain the optimal value for the objective function. It also engages with broader implications, such as the validation of the model as a reliable tool for groundwater management and policy formulation.

### 3.4. MODFLOW Transient Model Performance

Model calibration involves determining parameters and boundary conditions that align with past field observations within an acceptable margin of error. PEST iterations modify model parameter values to achieve the best objective function value. The primary goal is to construct the shallow aquifer by assuming that all surface water ultimately reaches the shallow aquifer via deep percolation. Therefore, total groundwater recharge is assumed to occur in the shallow aquifer. The NSE, MAE (mean absolute error, meters), and RMSE summary statistics for MODFLOW performance (illustrated in Figure 7) were proof of the model's reliability, particularly throughout the validation period, during which time performance was enhanced.

These results may validate the reliable results of the groundwater recharge dynamic from the SWAT model. A strong association exists between simulation and actual observations, as shown by the calibration and validation of the output parameters (groundwater level) results from the input parameters (such as groundwater recharge, storativity, hydraulic conductivity, and boundary condition). The validation model facilitates a rigorous and accurate assessment of the input parameters, thereby corroborating the compatibility of the employed hydrogeological model with the groundwater recharge observed in the study area.

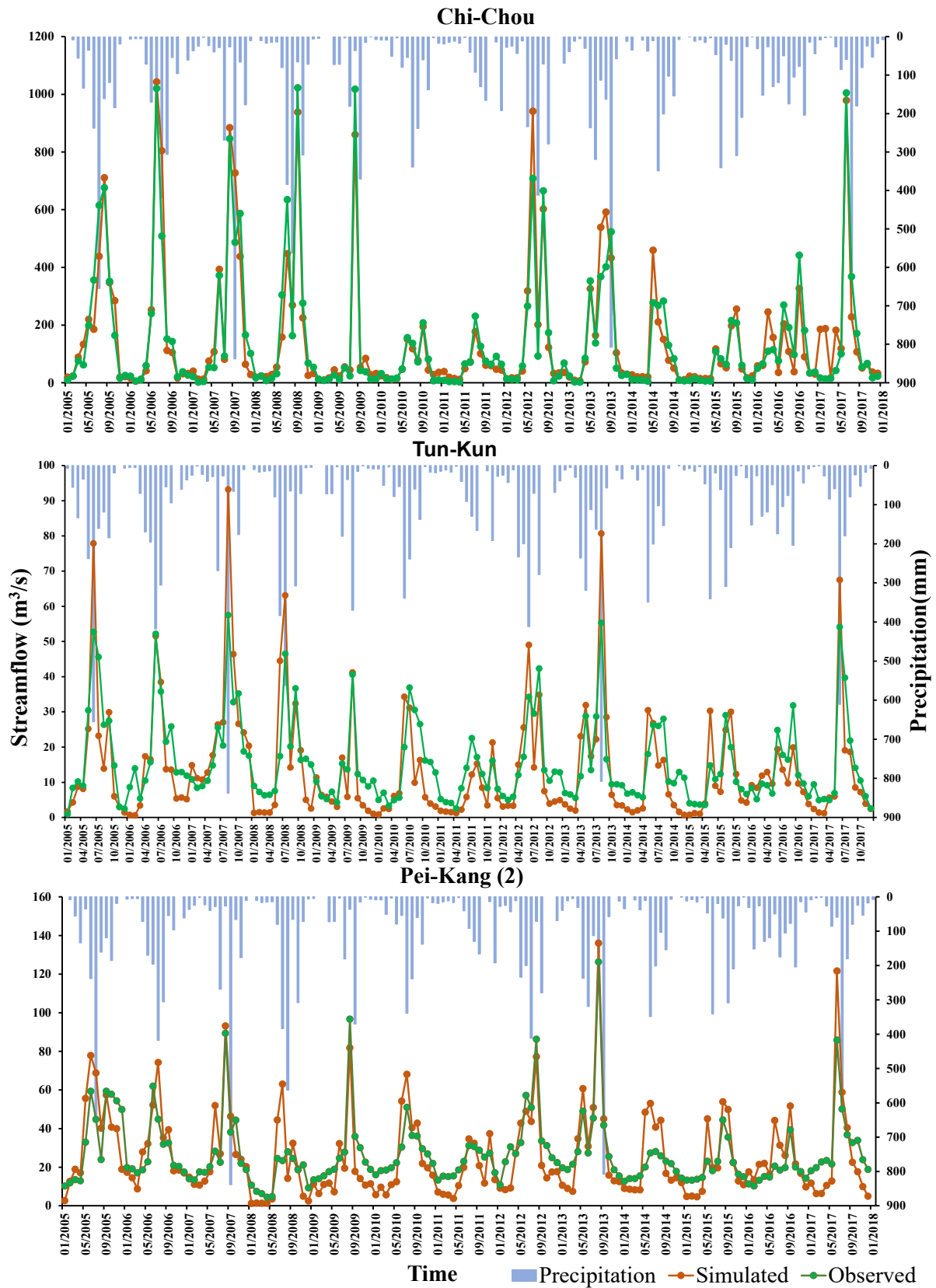


**Figure 5.** The correlation between monthly simulated, observed streamflow, and precipitation at Chi-Chou, Tun-Kun, and Pei-Kang (2) during the calibration (2005–2011) and validation time (2012–2017).

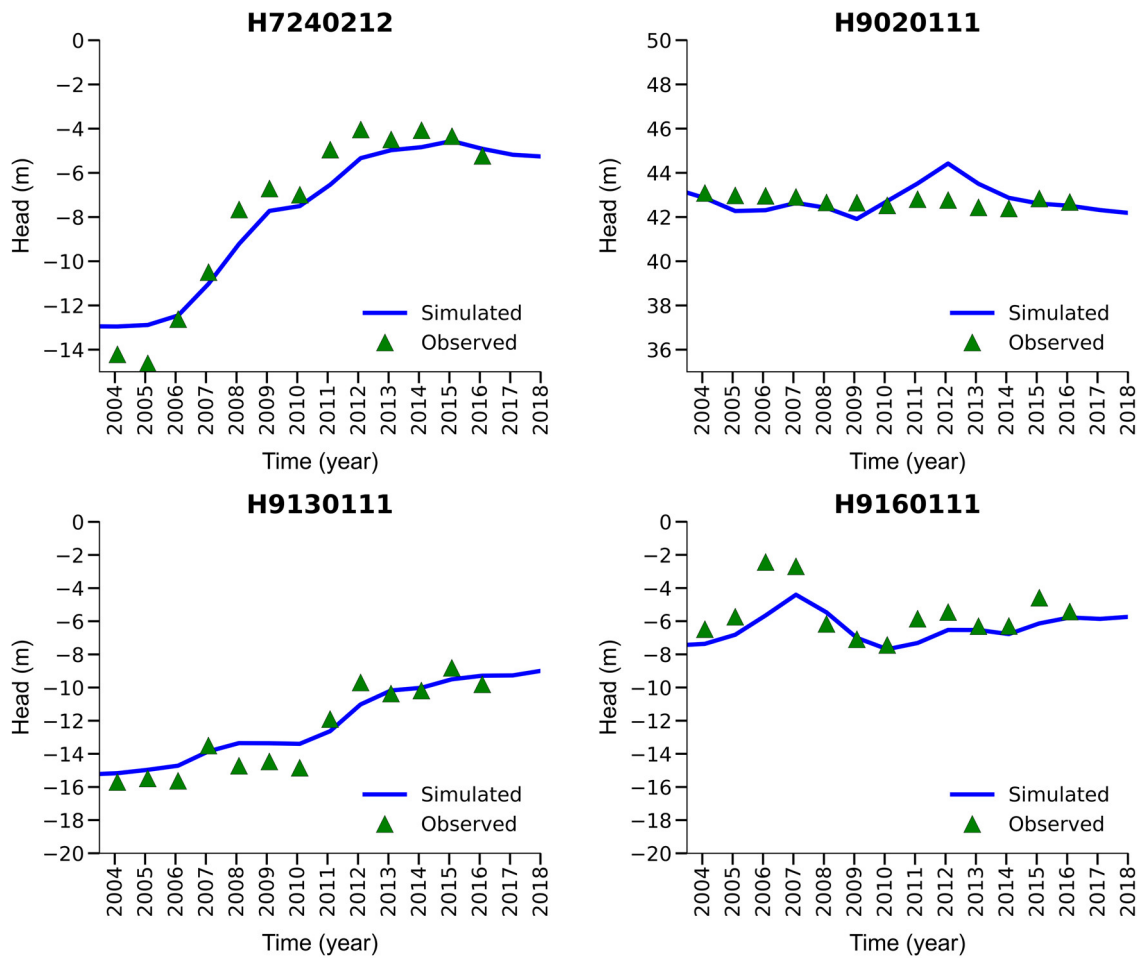


Figure 6. The simulated variation and observation data of groundwater level at four boreholes.

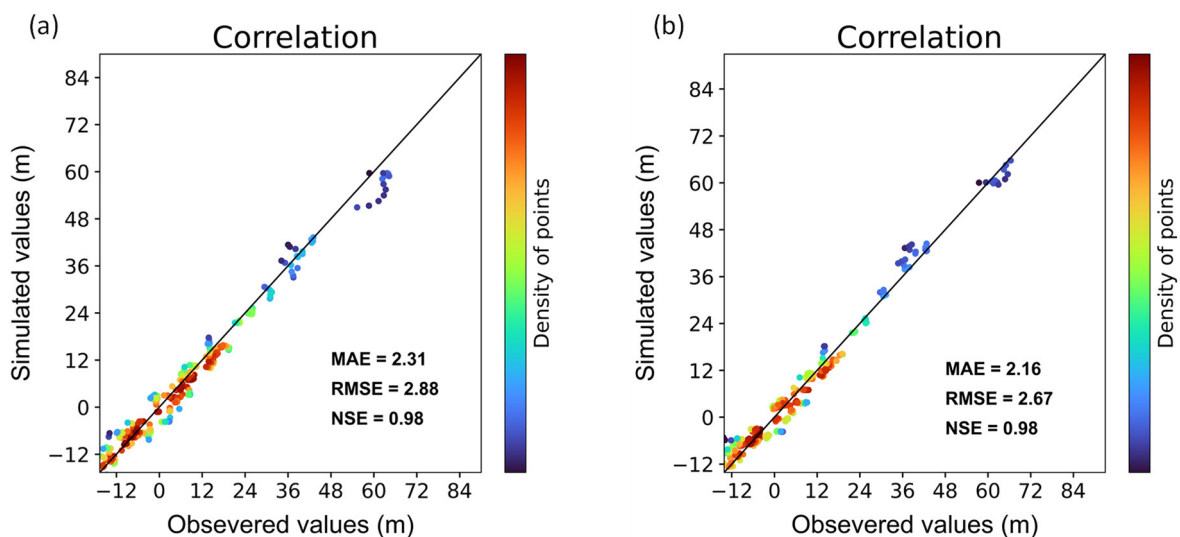


Figure 7. The correlation between the simulated and observed data during (a) calibration period (2005–2011) and (b) validation period (2012–2017).

### 3.5. Spatial Patterns of Groundwater Recharge Simulation

To make accurate projections of groundwater resource management, one needs to have an extensive comprehension of the geographically dispersed recharge process to precisely forecast the variations in recharge rate over time. The intricate relationship between

changing climatic factors and groundwater can be attributed to the recharge process and the interaction of surface water resources such as rivers and lakes. Therefore, assessing climate impact on groundwater supplies, precise projections of changes in primary climatic variables, and an accurate computation of the recharge rate are very important. This study proposes a technique based on HRUs that can explain the spatial aspect of groundwater recharge as percolation and the reflection through a lumped module in an individual sub-basin, contributing to the stream network as baseflow.

The analysis of the groundwater pattern revealed significant spatial variations across different geographic regions and has shown hotspots of groundwater potential among these HRUs (Figure 8). The results of this study revealed that the top fan area is the primary location for groundwater recharge, encompassing several high-potential recharge locations previously identified as sensitive areas for groundwater recharge by the Geological Survey and Mining Management Agency, Taiwan (indicated by the black polygon in Figure 8). Moreover, the rating levels of the recharge rate based on a probability-based model of aquifer vulnerability constructed by Chen et al. [58] are also depicted, with a high rating observed for the recharge rate in the proximal fan. Therefore, this study has identified several highly recharge-sensitive areas, caught up to almost all areas compared with the findings of the references, and provided a comprehensive understanding of the spatial distribution of groundwater recharge. This approach enables stakeholders and decision-makers to identify areas with higher or lower groundwater recharge rates and develop effective strategies for preserving and managing water resources.

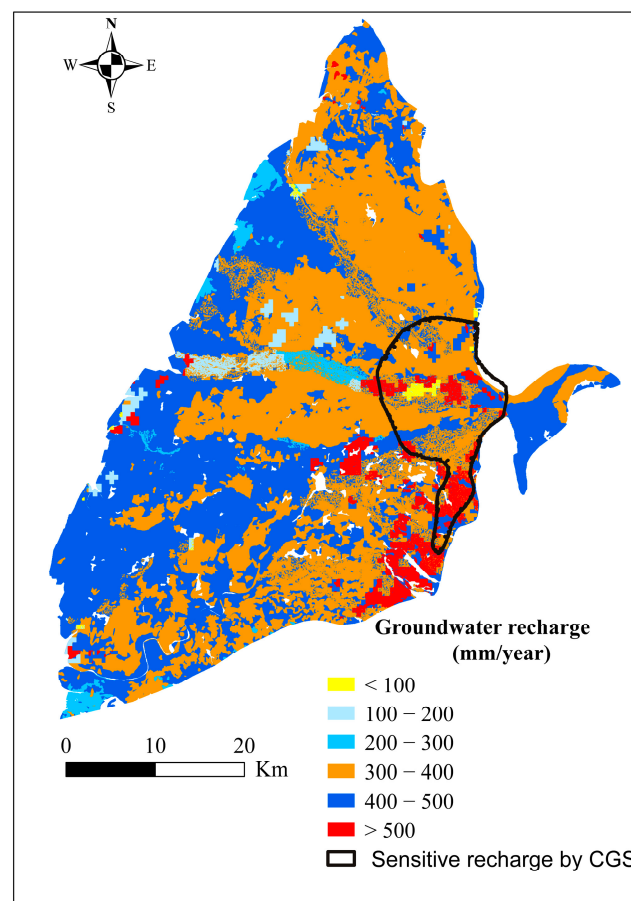


**Figure 8.** Annual recharge rate in CRAF.

In evaluating the mechanism of groundwater recharge, it is influenced by a complex interplay of sophisticated parameters and multiple circumstances, such as moist bulk density and water capacity. The quantification of the drainage systems to capture

stormwater runoff depends on the kind of land use, soil type, and moisture in the soil. The parameters, such as SOL\_BD (soil bulk density) and SOL\_AWC (soil available water capacity), also play a significant role in enhancing the accuracy of percolation estimation after analyzing the parameter sensitivity during calibration. The unsaturated zone soils often exhibit heterogeneity, characterized by layered sands, silts, and clays, resulting in non-uniform moisture distribution. Even areas with similar soil characteristics can experience significant differences in recharge rates due to topographical influences, leading to localized depressions that concentrate the water supply. Shallow groundwater levels also impose constraints on recharge by regulating the quantity of infiltrating water into the soil. Last but not least, anthropogenic activities, particularly urbanization, significantly impact recharge rates through increased impervious cover and modified water distribution systems. Therefore, the delineation of distinct HRUs based on their unique hydrological characteristics and responses offers a framework for elucidating the spatial heterogeneity of groundwater recharge across diverse regions. This approach enhances the accuracy and depth of knowledge regarding groundwater recharge dynamics, providing valuable insights for sustainable water resource management and land-use planning strategies in various geographical contexts.

### 3.6. Temporal Variability of Groundwater Recharge Scenarios Simulation

The potential impacts of climate change on groundwater recharge rates and supplies underscore the need for effective water resource management and long-term planning. Capturing spatial and temporal data pertaining to groundwater recharge is crucial for informed decision-making. The simulative data analysis offers substantial insights into the temporal variability of groundwater recharge, such as this study using the MIROC5 projection under the baseline and four RCP scenarios. Such an examination is imperative for the global scientific community as it aids in comprehending the potential impacts of climate change on groundwater resources, hence assisting in effective resource management and strategic planning.

In comparison with previous research, Wang et al. [6] estimated groundwater recharge amounts in the same areas that varied from  $0.549 \times 10^9$  to  $1.189 \times 10^9$  ( $\text{m}^3/\text{year}$ ) based on the stable baseflow approach and under the AR4 climate change scenario. Additionally, the Central Geological Survey, Taiwan, estimated an annual amount of groundwater recharge of approximately  $1.312 \times 10^9$  ( $\text{m}^3/\text{year}$ ) for the study area by combining geophysics and geochemical methods (Ministry of Economic Affairs, 2014). Although many studies using a variety of methodologies have attempted to estimate groundwater recharge in the region, the majority of these studies only offer an average of groundwater recharge over an extended period. However, differing from other methods, the model proposed herein integrates atmospheric and surface water interactions, providing not only annual estimates of groundwater recharge but also specifying values for each HRU. This precision is paramount in planning and management, allowing for adaptation to varying scenarios and reinforcing resilience against climate change. The results demonstrate groundwater recharge volumes and rates during the baseline period, ranging from  $0.650 \times 10^9$  to  $1.190 \times 10^9$  ( $\text{m}^3/\text{year}$ ). Projections for the future indicate groundwater recharge scenarios for the CRAF varying from approximately  $0.543 \times 10^9$  to  $1.555 \times 10^9$  ( $\text{m}^3/\text{year}$ ), contingent upon extreme events, such as the dry and wet years. These projections, in agreement with extant empirical research, offer a more refined approach by accounting for hydrologic response variability at the sub-basin scale, thus providing a detailed framework for assessing the potential impacts of climate variability and change.

This study analyzed the impact of future groundwater recharge scenarios on the study area in terms of near-term (2021–2040), mid-term (2041–2060, 2061–2080), and long-term (2081–2100) effects. The impact rate of each scenario was determined by calculating the percentage change in effect amount relative to the baseline quantity, as shown in Figure 9. This study aimed to determine the potential range of impact rates of climate change on

groundwater recharge in the study area from the 2020s to the 2100s under four scenarios, including identifying the maximum and minimum recharge rates.

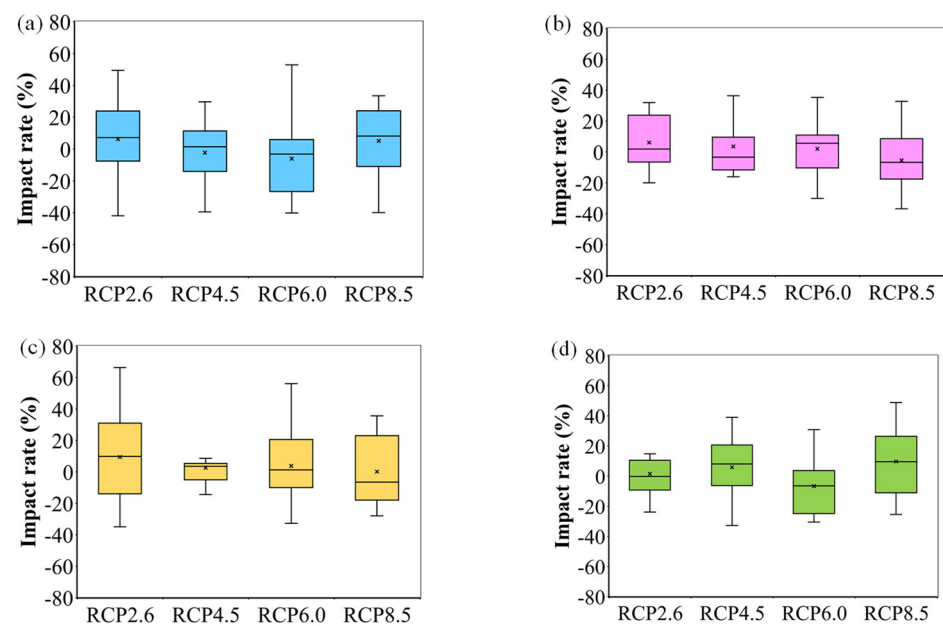


**Figure 9.** The impact rate of four RCPs' groundwater recharge against the baseline quantity for (a) near-term (2021–2040), (b) mid-term (2041–2060), (c) mid-term (2061–2080), and (d) long-term (2081–2100) periods. The color schemes indicate the different predicted periods.

In the initial time frame, it is discernible that the RCP6.0 scenario presents the most pronounced increase in groundwater recharge at 52.86%, with RCP2.6 and RCP8.5 following at 49.74% and 33.50% respectively. The least increase is noted under the RCP4.5 scenario at 29.67%. Conversely, each scenario exhibits a comparable percentage decrease in groundwater recharge, with values oscillating between  $-39.85\%$  (RCP8.5) and  $-41.92\%$  (RCP2.6). Upon progression to the mid-term period, a noticeable shift in the groundwater recharge pattern occurs. The RCP4.5 scenario depicts the most substantial percentage increase at 51.86%, trailed by RCP6.0 and RCP8.5 at 35.28% and 32.75% respectively. RCP2.6 yields the lowest increase at 31.96%. Intriguingly, all scenarios signify a diminished percentage decrease in groundwater recharge relative to the near-term duration, with a range between  $-19.99\%$  (RCP2.6) and  $-36.78\%$  (RCP8.5).

The temporal window between 2061 and 2080 witnesses RCP2.6 leading in percentage increase in groundwater recharge (66.36%), succeeded by RCP6.0 (56.11%) and RCP8.5 (35.67%). RCP4.5 displays the smallest percentage increase (29.68%). Simultaneously, there is a consistent reduction across all scenarios in the percentage decrease in groundwater recharge compared with the mid-term period, with values spanning from  $-23.05\%$  (RCP4.5) to  $-34.96\%$  (RCP2.6). In the long-term span, RCP8.5 surfaces as the scenario with the greatest percentage increase in groundwater recharge (48.92%), followed closely by RCP2.6 (47.62%) and then RCP4.5 (39.02%). RCP6.0 exhibits the least percentage increase (30.89%). Similarly, each scenario highlights a decrease in the percentage reduction in groundwater recharge relative to the preceding period, varying from  $-23.85\%$  (RCP2.6) to  $-32.76\%$  (RCP4.5).

The results illustrate that the impact rate of climate change on groundwater recharge varies across different scenarios and over time. Some scenarios show an increase in groundwater recharge, while others decrease it. However, all the scenarios indicate a reduction in groundwater recharge impact rates over time, indicating that the impact of climate change on groundwater recharge may reduce in the long-term.

A comparative analysis performed by Wang et al. [6] revealed that the impact of climate change on groundwater systems may be positive, with an increase of 32.6% or a decrease of 28.9% on average. However, this perspective, under the AR4 report, compared with the

findings presented herein, based on the more recent AR5 framework, elucidate a complex and varied impact rate of climate change on groundwater recharge across more historical data and progress worldwide. The divergence in results highlights the intricate nature of climate change and underscores that its impact on groundwater systems is multifaceted, subject to change, and dependent on the selected framework and assumptions. This detailed examination of temporal variability is instrumental in advancing our understanding of the impact of climate change on groundwater recharge rates and supplies. It emphasizes the necessity for strategic water resource management and extensive planning. The results not only provide guidance for local applications but also make a substantial contribution to the global understanding of the impact of climate change on groundwater recharge. As such, the presented study can inform global efforts for effective water resource management under varying future climatic conditions. Through the incorporation of high-resolution spatial and temporal data, a more nuanced understanding of groundwater dynamics is offered.

#### 4. Conclusions

The global community grapples with the pressing challenges of sustainable groundwater management, as these reserves play a pivotal role in supporting ecosystems and human livelihoods, especially against the backdrop of unpredictable climate change. The application of SWAT-MODFLOW models has been widely used to address these issues worldwide. Nevertheless, the uniqueness of this study lies not in the use of the models themselves but in the comprehensive application and combination of these models to assess the potential impacts of climate change on groundwater recharge. The approach is particularly valuable for regions similar to the CRAF, Taiwan, but the methodology can also be extrapolated to understand the effects of climate change in other varied geographic contexts. The objectives of this study were successfully met, as the models were able to estimate streamflow discharge and assess the potential impact of climate change scenarios on groundwater recharge in the future. The calibrated model's credibility is bolstered by validation and characterized by strong statistical performance in capturing watershed responses. Moreover, the automatic PEST calibration in MODFLOW effectively captures groundwater head temporal patterns and highlights the importance of optimizing boreholes and methodologies for uncertainty management. This role is particularly accentuated in the context of this study, which underscores how modeling underpins evidence-based decision-making processes within the realm of water resource management. The results also revealed that the spatial distribution of the recharge rate mainly occurs in the proximal fan area, encompassing several high-potential recharge locations with previously delineated sensitive areas for groundwater recharge in literature. The spatial distribution insights, while rooted in the study area, set the stage for researchers elsewhere to refine their understanding of high-potential recharge locations. The temporal variability analyses shed light on the evolving impacts of climate change on groundwater recharge, emphasizing the need for proactive and strategic global water resource planning. While some scenarios show an increase in groundwater recharge, all scenarios indicate a decrease in the impact of climate change on groundwater recharge over time. These results suggest that the impact of climate change on groundwater recharge may decrease in the long-term, although the rate of this decrease may vary across different scenarios. Through its detailed methodology and findings, this research fortifies the existing body of knowledge, refining methods to project groundwater recharge variability amidst shifting climate scenarios. The incorporation of high-resolution data provides a blueprint for other researchers to attain a deeper grasp on groundwater dynamics and its susceptibility to climatic changes. The employment of the top-ranked MIROC5 projection of GCMs in our study sets a benchmark, introducing an avenue to evaluate further GCM projections for an exhaustive appraisal. In conclusion, the insights gleaned from this research necessitate concerted actions from policy-makers and stakeholders. By aligning our groundwater management strategies with the ever-evolving climate paradigms, we can aspire for a sustainable coexistence with our environment.

**Author Contributions:** Conceptualization, S.-J.W., P.-Y.C. and T.-M.-L.N.; methodology, S.-J.W., P.-Y.C. and T.-M.-L.N.; software, T.-M.-L.N.; validation, T.-M.-L.N., S.-J.W. and P.-Y.C.; formal analysis, T.-M.-L.N.; investigation, T.-M.-L.N.; resources, S.-J.W. and P.-Y.C.; data curation, S.-J.W. and P.-Y.C.; writing—original draft preparation, T.-M.-L.N.; Writing - review & editing, S.-J.W.; visualization, T.-M.-L.N.; supervision, S.-J.W. and P.-Y.C., project administration S.-J.W.; funding acquisition, S.-J.W. All authors have read and agreed to the published version of the manuscript.

**Funding:** This study was supported by the Ministry of Science and Technology, Taiwan, under grants MOST 110-2116-M-008-003 and MOST 111-2116-M-008-007.

**Data Availability Statement:** The climate scenarios were collected from the website [https://tccip.ncdr.nat.gov.tw/index\\_eng.aspx](https://tccip.ncdr.nat.gov.tw/index_eng.aspx) (accessed on 27 January 2024). Account registration is required to collect the data.

**Acknowledgments:** The authors would like to thank the institutes to provide the data. The hydrological observation data were provided by Taiwan Water Resources Agency and Taiwan Central Weather Administration while the future climate data are provided by The Taiwan Climate Change Projection Information and Adaptation Knowledge Platform (TCCIP).

**Conflicts of Interest:** The authors declare that they have no known competing financial interests or personal relationships that could have appeared to influence the work reported in this paper.

## References

- Liesch, T.; Wunsch, A. Aquifer responses to long-term climatic periodicities. *J. Hydrol.* **2019**, *572*, 226–242. [[CrossRef](#)]
- Mach, K.J.; Mastrandrea, M.D.; Bilir, T.E.; Field, C.B. Understanding and responding to danger from climate change: The role of key risks in the IPCC AR5. *Clim. Chang.* **2016**, *136*, 427–444. [[CrossRef](#)]
- Awan, U.K.; Ismaeel, A. A new technique to map groundwater recharge in irrigated areas using a SWAT model under changing climate. *J. Hydrol.* **2014**, *519*, 1368–1382. [[CrossRef](#)]
- Hu, B.; Teng, Y.; Zhang, Y.; Zhu, C. Review: The projected hydrologic cycle under the scenario of 936 ppm CO<sub>2</sub> in 2100. *Hydrogeol. J.* **2018**, *27*, 31–53. [[CrossRef](#)]
- Pulido-Velazquez, D.; Collados-Lara, A.-J.; Alcalá, F.J. Assessing impacts of future potential climate change scenarios on aquifer recharge in continental Spain. *J. Hydrol.* **2018**, *567*, 803–819. [[CrossRef](#)]
- Wang, S.-J.; Lee, C.-H.; Yeh, C.-F.; Choo, Y.F.; Tseng, H.-W. Evaluation of Climate Change Impact on Groundwater Recharge in Groundwater Regions in Taiwan. *Water* **2021**, *13*, 1153. [[CrossRef](#)]
- Karki, R.; Srivastava, P.; Kalin, L. Evaluating climate change impacts in a heavily irrigated karst watershed using a coupled surface and groundwater model. *J. Hydrol. Reg. Stud.* **2023**, *50*, 101565. [[CrossRef](#)]
- Hersi, N.A.; Mulungu, D.M.; Nobert, J. Groundwater recharge estimation under changing climate and land use scenarios in a data-scarce Bahi (Manyoni) catchment in Internal Drainage Basin (IDB), Tanzania using Soil and Water Assessment Tool (SWAT). *Groundw. Sustain. Dev.* **2023**, *22*, 100957. [[CrossRef](#)]
- Oki, T.; Kanae, S. Global Hydrological Cycles and World Water Resources. *Science* **2006**, *313*, 1068–1072. [[CrossRef](#)] [[PubMed](#)]
- Postel, S.L.; Daily, G.C.; Ehrlich, P.R. Human Appropriation of Renewable Fresh Water. *Science* **1996**, *271*, 785–788. [[CrossRef](#)]
- Vörösmarty, C.J.; Green, P.; Salisbury, J.; Lammers, R.B. Global Water Resources: Vulnerability from Climate Change and Population Growth. *Science* **2000**, *289*, 284–288. [[CrossRef](#)] [[PubMed](#)]
- Camporese, M.; Paniconi, C.; Putti, M.; Salandín, P. Ensemble Kalman filter data assimilation for a process-based catchment scale model of surface and subsurface flow. *Water Resour. Res.* **2009**, *45*, W10421. [[CrossRef](#)]
- Sophocleous, M. Interactions between groundwater and surface water: The state of the science. *Hydrogeol. J.* **2002**, *10*, 348. [[CrossRef](#)]
- Winter, T.C. *Groundwater Surface Water: A Single Resource*; U.S. Geological Survey Circular 1139; U.S. Geological Survey: Denver, CO, USA, 1998.
- Kollet, S.J.; Maxwell, R.M. Integrated surface–groundwater flow modeling: A free-surface overland flow boundary condition in a parallel groundwater flow model. *Adv. Water Resour.* **2006**, *29*, 945–958. [[CrossRef](#)]
- Markstrom, S.L.; Niswonger, R.G.; Regan, R.S.; Prudic, D.E.; Barlow, P.M. GSFLOW—Coupled Ground-Water and Surface-Water Flow Model Based on the Integration of the Precipitation-Runoff Modeling System (PRMS) and the Modular Ground-Water Flow Model (MODFLOW-2005). *US Geol. Surv. Tech. Methods* **2008**, *6*, 240.
- Kim, N.W.; Chung, I.M.; Won, Y.S.; Arnold, J.G. Development and application of the integrated SWAT–MODFLOW model. *J. Hydrol.* **2008**, *356*, 1–16. [[CrossRef](#)]
- Therrien, R.; McLaren, R.; Sudicky, E.; Panday, S. *HydroGeoSphere: A Three-Dimensional Numerical Model Describing Fully-Integrated Subsurface and Surface Flow and Solute Transport*; Groundwater Simulations Group, University of Waterloo: Waterloo, ON, USA, 2010.
- Diersch, H.-J.G. *FEFLOW: Finite Element Modeling of Flow, Mass and Heat Transport in Porous and Fractured Media*, 1st ed.; Springer: Berlin/Heidelberg, Germany, 2013. [[CrossRef](#)]

20. Gassman, P.W.; Reyes, M.R.; Green, C.H.; Arnold, J.G. The Soil and Water Assessment Tool: Historical Development, Applications, and Future Research Directions. *Trans. ASABE* **2007**, *50*, 1211–1250. [[CrossRef](#)]
21. Neitsch, S.L.; Arnold, J.G.; Kiniry, J.R.; Williams, J.R. *Soil and Water Assessment Tool Theoretical Documentation Version 2009*; Texas Water Resources Institute: College Station, TX, USA, 2011; Available online: <https://hdl.handle.net/1969.1/128050> (accessed on 10 August 2022).
22. Hashemi, F.; Olesen, J.E.; Dalgaard, T.; Børgesen, C.D. Review of scenario analyses to reduce agricultural nitrogen and phosphorus loading to the aquatic environment. *Sci. Total. Environ.* **2016**, *573*, 608–626. [[CrossRef](#)]
23. Hossard, L.; Chopin, P. Modelling agricultural changes and impacts at landscape scale: A bibliometric review. *Environ. Model. Softw.* **2019**, *122*, 104513. [[CrossRef](#)]
24. Mannschatz, T.; Wolf, T.; Hülsmann, S. Nexus Tools Platform: Web-based comparison of modelling tools for analysis of water-soil-waste nexus. *Environ. Model. Softw.* **2016**, *76*, 137–153. [[CrossRef](#)]
25. Wei, F.; Grubestic, T.H.; Bishop, B.W. Exploring the GIS Knowledge Domain Using CiteSpace. *Prof. Geogr.* **2014**, *67*, 374–384. [[CrossRef](#)]
26. Niswonger, R.G.; Panday, S.; Ibaraki, M. MODFLOW-NWT, a Newton formulation for MODFLOW-2005. *US Geol. Surv. Tech. Methods* **2011**, *6*, 44.
27. Sophocleous, M.; Koelliker, J.; Govindaraju, R.; Birdie, T.; Ramireddygar, S.; Perkins, S. Integrated numerical modeling for basin-wide water management: The case of the Rattlesnake Creek basin in south-central Kansas. *J. Hydrol.* **1999**, *214*, 179–196. [[CrossRef](#)]
28. Sanz, D.; Castaño, S.; Cassiraga, E.; Sahuquillo, A.; Gómez-Alday, J.J.; Peña, S.; Calera, A. Modeling aquifer–river in-teractions under the influence of groundwater abstraction in the Mancha Oriental System (SE Spain). *Hydrogeol. J.* **2011**, *19*, 475–487. [[CrossRef](#)]
29. Stefania, G.A.; Rotiroti, M.; Fumagalli, L.; Simonetto, F.; Capodaglio, P.; Zanotti, C.; Bonomi, T. Modeling groundwater/surface-water interactions in an Alpine valley (the Aosta Plain, NW Italy): The effect of groundwater abstraction on surface-water resources. *Hydrogeol. J.* **2017**, *26*, 147–162. [[CrossRef](#)]
30. Bailey, R.T.; Wible, T.C.; Arabi, M.; Records, R.M.; Ditty, J. Assessing regional-scale spatio-temporal patterns of groundwater–surface water interactions using a coupled SWAT-MODFLOW model. *Hydrol. Process.* **2016**, *30*, 4420–4433. [[CrossRef](#)]
31. Liu, W.; Park, S.; Bailey, R.T.; Molina-Navarro, E.; Andersen, H.E.; Thodsen, H.; Nielsen, A.; Jeppesen, E.; Jensen, J.S.; Trolle, D. Quantifying the streamflow response to groundwater abstractions for irrigation or drinking water at catchment scale using SWAT and SWAT-MODFLOW. *Environ. Sci. Eur.* **2020**, *32*, 1–25. [[CrossRef](#)]
32. Mote, P.W.; Abatzoglou, J.T.; Kunkel, K.E. Climate. In *Climate Change in the Northwest*; NCA Regional Input Reports; Dalton, M.M., Mote, P.W., Snover, A.K., Eds.; Island Press: Washington, DC, USA, 2013. [[CrossRef](#)]
33. Fu, G.; Crosbie, R.S.; Barron, O.; Charles, S.P.; Dawes, W.; Shi, X.; Van Niel, T.; Li, C. Attributing variations of temporal and spatial groundwater recharge: A statistical analysis of climatic and non-climatic factors. *J. Hydrol.* **2018**, *568*, 816–834. [[CrossRef](#)]
34. McKenna, O.P.; Sala, O.E. Groundwater recharge in desert playas: Current rates and future effects of climate change. *Environ. Res. Lett.* **2017**, *13*, 014025. [[CrossRef](#)]
35. Maxwell, R.M.; Condon, L.E.; Kollet, S.J. A high-resolution simulation of groundwater and surface water over most of the continental US with the integrated hydrologic model ParFlow v3. *Geosci. Model Dev.* **2015**, *8*, 923–937. [[CrossRef](#)]
36. O’neill, S.; Williams, H.T.P.; Kurz, T.; Wiersma, B.; Boykoff, M. Dominant frames in legacy and social media coverage of the IPCC Fifth Assessment Report. *Nat. Clim. Chang.* **2015**, *5*, 380–385. [[CrossRef](#)]
37. Parry, M.L.; Canziani, O.; Palutikof, J.; Van der Linden, P.; Hanson, C. *Climate Change 2007-Impacts, Adaptation and Vulnerability: Working Group II Contribution to the Fourth Assessment Report of the IPCC*; Cambridge University Press: Cambridge, UK, 2007; Volume 4.
38. Srinivasan, V.; Lele, S. From groundwater regulation to integrated water management. *Econ. Polit. Wkly.* **2017**, *52*, 107–114.
39. Tweed, S.; Leblanc, M.; Cartwright, I.; Favreau, G.; Leduc, C. Arid zone groundwater recharge and salinisation processes; an example from the Lake Eyre Basin, Australia. *J. Hydrol.* **2011**, *408*, 257–275. [[CrossRef](#)]
40. Barron, O.; Crosbie, R.; Charles, S.; Dawes, W.; Ali, R.; Evans, W.; Cresswell, R.; Pollock, D.; Hodgson, G.; Currie, D. *Climate Change Impact on Groundwater Resources in Australia Waterlines Report*; National Water Commission: Canberra, Australia, 2011.
41. Bellot, J.; Chirino, E. Hydrobal: An eco-hydrological modelling approach for assessing water balances in different vegetation types in semi-arid areas. *Ecol. Model.* **2013**, *266*, 30–41. [[CrossRef](#)]
42. Touhami, I.; Chirino, E.; Andreu, J.; Sánchez, J.; Moutahir, H.; Bellot, J. Assessment of climate change impacts on soil water balance and aquifer recharge in a semiarid region in south east Spain. *J. Hydrol.* **2015**, *527*, 619–629. [[CrossRef](#)]
43. Meixner, T.; Manning, A.H.; Stonestrom, D.A.; Allen, D.M.; Ajami, H.; Blasch, K.W.; Brookfield, A.E.; Castro, C.L.; Clark, J.F.; Gochis, D.J.; et al. Implications of projected climate change for groundwater recharge in the western United States. *J. Hydrol.* **2016**, *534*, 124–138. [[CrossRef](#)]
44. Flint, L.; Flint, A. *California Basin Characterization Model: A Dataset of Historical and Future Hydrologic Response to Climate Change*; US Geological Survey Data Release: Reston, VA, USA, 2014. [[CrossRef](#)]
45. Bhanja, S.N.; Rodell, M.; Li, B.; Saha, D.; Mukherjee, A. Spatio-temporal variability of groundwater storage in India. *J. Hydrol.* **2017**, *544*, 428–437. [[CrossRef](#)] [[PubMed](#)]

46. Jyrkama, M.I.; Sykes, J.F. The impact of climate change on spatially varying groundwater recharge in the grand river watershed (Ontario). *J. Hydrol.* **2007**, *338*, 237–250. [[CrossRef](#)]
47. Moeck, C.; Grech-Cumbo, N.; Podgorski, J.; Bretzler, A.; Gurdak, J.J.; Berg, M.; Schirmer, M. A global-scale dataset of direct natural groundwater recharge rates: A review of variables, processes and relationships. *Sci. Total. Environ.* **2020**, *717*, 137042. [[CrossRef](#)]
48. Jia, Y.-P. Hydrogeological Structure of the Southern Wing of Choushui River Alluvial Fan. In Proceedings of the Workshop on Groundwater and Hydrogeology of the Choushui River Alluvial Fan, Taipei city, Taiwan, 2 September 1996; pp. 113–125.
49. Hsu, H. Investigation of Groundwater Recharge Estimation—A Case Study in Choushui River Alluvial Fan. Master’s Thesis, National Taiwan University, Taipei City, Taiwan, 2010. Available online: <https://hdl.handle.net/11296/hc8xc2> (accessed on 27 January 2024).
50. Ke, K.-Y. Application of an integrated surface water-groundwater model to multi-aquifers modeling in Choushui River alluvial fan, Taiwan. *Hydrol. Process.* **2012**, *28*, 1409–1421. [[CrossRef](#)]
51. Ray, M.; Simpson, B. *Agricultural Adaptation to Climate Change in the Sahel: Profiles of Agricultural Management Practices*; Tetra Tech ARD Report; USAID: Washington, DC, USA, 2014; p. 60.
52. USDA. Section 4: Hydrology. In *National Engineering Handbook*; USDA: Washington, DC, USA, 1972.
53. Ministry of Economic Affairs. Designation Plan for Groundwater Recharge Geologically Sensitive Areas: G0001 Choushui River Alluvial Fan. 2014. Available online: <https://www.gsmma.gov.tw/nss/p/H001d2> (accessed on 27 January 2024).
54. Abbaspour, K.C.; Rouholahnejad, E.; Vaghefi, S.; Srinivasan, R.; Yang, H.; Kløve, B. A continental-scale hydrology and water quality model for Europe: Calibration and uncertainty of a high-resolution large-scale SWAT model. *J. Hydrol.* **2015**, *524*, 733–752. [[CrossRef](#)]
55. Ranganathan, A. The levenberg-marquardt algorithm. *Tutorial LM Algorithm* **2004**, *11*, 101–110.
56. Lin, C.-Y.; Tung, C.-P. Procedure for selecting GCM datasets for climate risk assessment. *Terr. Atmos. Ocean. Sci.* **2017**, *28*, 43–55. [[CrossRef](#)]
57. Lin, X.-L.; Lin, S.-Y.; Tong, Y.-X. Statistical Downscaling Rainfall Data Production Record AR5 (4.0 Edition). Taiwan Climate Change Projection and Adaptation Knowledge Platform. 2021. Available online: [https://tccip.ncdr.nat.gov.tw/upload/data\\_profile/20200117105955.pdf](https://tccip.ncdr.nat.gov.tw/upload/data_profile/20200117105955.pdf) (accessed on 10 August 2022).
58. Chen, S.-K.; Jang, C.-S.; Peng, Y.-H. Developing a probability-based model of aquifer vulnerability in an agricultural region. *J. Hydrol.* **2013**, *486*, 494–504. [[CrossRef](#)]

**Disclaimer/Publisher’s Note:** The statements, opinions and data contained in all publications are solely those of the individual author(s) and contributor(s) and not of MDPI and/or the editor(s). MDPI and/or the editor(s) disclaim responsibility for any injury to people or property resulting from any ideas, methods, instructions or products referred to in the content.